Fields of optical waveguides as waves in free space

S. V. Kukhlevsky and G. Nyitray
Department of Physics, University of Pecs, Ifjusag u. 6, Pecs 7624, Hungary

V. L. Kantsyrev
Department of Physics/220, University of Nevada, Reno, Nevada 89557-0058
(Received 17 December 2000; published 16 July 2001)

It is shown by using the scalar diffraction theory and the method of images that the arbitrary field confined by the optical waveguide can be generated in free space by the appropriate light source. The correspondence between the guided and free-space waves is illustrated using several particular fields, such as the diffraction-free, self-imaging, ultra-short, solitonlike, partially coherent waves and laser fractals. In opposition to the eigenmode theory of waveguides, the field at the guide entrance can satisfy neither the guide wave-equation nor the boundary conditions.

DOI: 10.1103/PhysRevE.64.026603 PACS number(s): 42.79.Gn, 42.25.Bs

I. INTRODUCTION

Bounded optical fields confined by multiple internal reflections at the waveguide boundaries and optical beams propagating in free space are attracting continuous interest because of their importance for basic physics and applications in technology. This subject has been known for decades and many ways to treat the problem can be found in the literature. The behavior of such waves is governed by Maxwell's wave equations with the boundary conditions imposed. According to the conventional theory of optical waveguides (solving a boundary condition problem), a wave arriving to the guide entrance and satisfying the wave equation and the boundary conditions of the guide propagates without diffractive broadening through the optical conduit as a superposition of the well-known waveguide eigenmodes. In free space the wave equation and the boundary conditions are different from that of the waveguide. A wave propagates between different locations in free space as the optical beam that diffracts and broadens. Up to now it was commonly thought that the fields confined by optical waveguides are different in principle from the optical beams propagating in free space.

In this paper we show using the scalar diffraction theory and the method of images that the arbitrary field confined by the optical waveguide can be generated in free space by the appropriate light source. The guided field can be produced in free-space provided an appropriate launch pattern containing multiple virtual sources can be constructed. In opposition to the conventional theory of waveguides, the field at the guide entrance can satisfy neither the guide wave equation nor the boundary conditions. That gives possibility to considering not only the mode-matched waves, but also the fields having more complicated spatial and temporal properties at the guide entrance. The correspondence between the guided and free-space waves is illustrated using several particular fields, such as the diffraction-free, self-imaging, ultrashort, solitonlike, partially coherent waves and laser fractals. Some of these fields have been found recently (diffraction-free beams and laser fractals [1–10]) and some many years ago (self-imaging, solitonlike, ultrashort, and partially coherent fields [11–14]). The fields are compared, where it is possible (mode-matched fields), to those obtained by solving a boundary condition problem.

II. GENERAL CONSIDERATION

Let us first consider, for the sake of simplicity, the propagation of waves through the plane waveguide (Fig. 1). The guide, which consists of a core and a cladding, is tapered with the taper angle γ. The complex index of refraction $n = n_r - i n_{im}$ changes abruptly from n_1 to n_2 at the guide boundary. Here n_{im} is the absorption index of the medium.

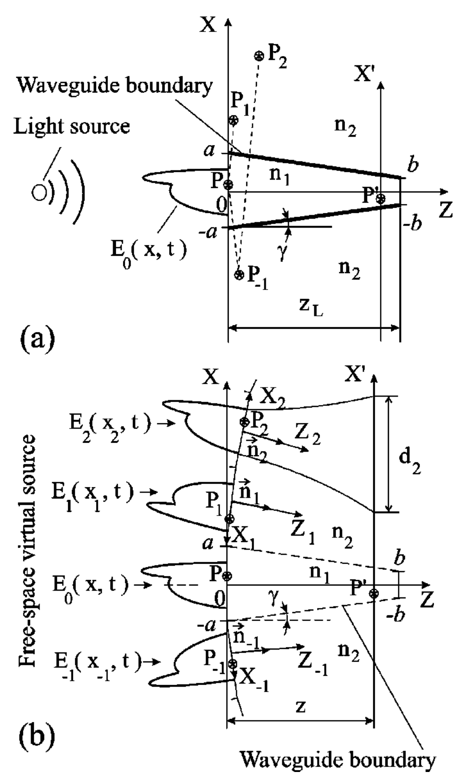

FIG. 1. (a) Propagation of the wave through the tapered optical waveguide. (b) Schematic diagram of the free-space virtual source.

We consider the guide of length z_L with the dimensions $2a$ and $2b$ of the entrance and exit, respectively. In the case of harmonic fields a wave $E_0(P,t)$ at the point $P(x,z)$ of the guide entrance ($x\in[-a,a]$ and $z=0$) is given by $E_0(P,t)=E_0(x)\exp\{i[-\omega t+\phi_0(x)]\}$, where x and z are the coordinates of the point P in the coordinate system (X,Z); ω and $\phi_0(x)$ are the wave frequency and the phase, respectively. In accordance with the Huygens-Fresnel principle, which is usually regarded as a form of the Helmholtz-Kirchhoff integral theorem, every point $P(x,z)$ of the wave $E_0(P,t)$ can be considered as the center of a secondary spherical wave. When the secondary wave reaches the core-cladding boundary, it is split into two waves: a transmitted (leaky) wave proceeding into the second medium and a reflected wave propagating back into the first medium. According to the method of images, the reflected secondary wave can be represented as a wave emerging from the respective point $P_1(x_1,z_1)$ of the free-space virtual source (Fig. 1). The amplitude and phase of the wave are determined by the Fresnel field reflectivity and the phase change associated with the reflection. The field $E_0(P,t)$, after m reflections, can be represented as the field (beam) $E'_m(P',t)$ emerged from the mth zone of the virtual source having the field distribution $E_m(P_m,t)$. The field distribution in this zone is given by $E_m(P_m,t)=R_mE_0(x_m)\exp[i(\phi_0(x_m)+\Delta\phi_m-\omega t)]$, where the amplitude and the phase are determined by the reflectivity $R_m=\Pi_{j=1}^{m}R_j(\Phi_j,n_1,n_2)$ and the phase change $\Delta\phi_m=\Sigma_{j=1}^{m}\Delta\phi_j(\Phi_j,n_1,n_2)$ for the m reflections. Here, $R_j(\Phi_j,n_1,n_2)$ and $\Delta\phi_j(\Phi_j,n_1,n_2)$ are, respectively, the Fresnel field reflectivity and the phase change for the beam $E'_j(P',t)$ emerged from the jth zone of the virtual source and reflected at the glancing angle Φ_j [15]. The field $E'_m(P',t)$ at a general point P' of the guide core is given by the Fresnel-Kirchhoff integral [16],

$$E'_m(P',t)=\frac{1}{\sqrt{2i\lambda}}\int_{x_m^{min}}^{x_m^{max}}\frac{\exp[ikr(P'_m,P_m)]}{r(P'_m,P_m)}\times(1+\cos\Theta_m)E_m(P_m,t)\,dx_m, \tag{1}$$

with $P_m=P(x_m,z_m)$ and $P'_m=P'(x'_m,z'_m)$, where (x_m,z_m) and (x'_m,z'_m) are the coordinates of the points P and P' in the coordinate system (X_m,Z_m), respectively. The points $P_m=P(x_m,z_m)$ are the images of the points $P=P(x,z)$. The transformation can be presented as the rotation, translation, and inversion of the coordinate system (X,Z),

$$\begin{pmatrix} x_m \\ z_m \end{pmatrix}=\begin{pmatrix} \cos(2m\gamma), & \pm(-1)^m\sin(2m\gamma) \\ \mp(-1)^m\sin(2m\gamma), & \cos(2m\gamma)\end{pmatrix}\begin{pmatrix} x_m^{t,i} \\ z_m^{t}\end{pmatrix}, \tag{2}$$

$$x_m^{t,i}=\left[x\mp a\left\{1+\cos(2m\gamma)-2(\delta_{1m}-1)\sum_{j=1}^{m-1}\cos(2j\gamma)\right\}\right]\times(-1)^m, \tag{3}$$

$$z_m^{t}=z-a\left[\sin(2m\gamma)-2(\delta_{1m}-1)\sum_{j=1}^{m-1}\sin(2j\gamma)\right]. \tag{4}$$

Here, $r(P'_m,P_m)$ is the distance between points P'_m and P_m; Θ_m is the angle that the line (P'_mP_m) makes with the unit normal $\vec{e}_m$ to the line $(x_m^{min}x_m^{max})$; λ is the wavelength; $[x_m^{min},x_m^{max}]$ is the mth zone; δ_{1m} is the Kronecker symbol; and the top and bottom signs are used for $x>0$ and $x<0$, respectively. It should be noted that absorption of the wave is determined by the imaginary part of the propagation constant $k=\omega n_1/c$ of Eq. (1). The total field $E'(P',t)$ at the point P' is found by summing the contributions from the M zones of the virtual source

$$E'(P',t)=\sum_{m=|-M|}^{M}E'_m(P',t), \tag{5}$$

where M is the number of zones (beams) that contribute the energy into the field $E'(P',t)$. The number M depends on the direction of propagation and the divergence angle of the beams $E'_m(P',t)$. These two parameters are determined by the value γ and the transverse dimensions $d_m(\lambda,a,z)$ of the beams $E'_m(P',t)$. For the tapered and plane-parallel guides, an analysis of Eq. (5) shows that the arbitrary wave $E_0(P,t)$ propagates down the guides as the superposition of the "transient" modes $E'_m(P',t)$ that diffract in the off-axis direction and interfere with each other. This result is more general in comparison to the predictions of the conventional theory of waveguides (solving a boundary condition problem for the plane-parallel guides). According to the conventional theory, a wave arriving to the guide entrance and satisfying the wave equation and the boundary conditions propagates through the optical conduit as a superposition of the steady-state fields (eigenmodes). In our consideration even an eigenmode of the plane-parallel guide propagates through the guide as the superposition of the transient modes.

The new method can be extended to the waveguide having a gradient-refraction index. In this case the usual approach based on the representation of the graded index medium by the steplike refraction index multiguide structure should be used. For the transmitted (leaky) wave proceeding into the second medium the Fresnel field reflectivity R_j and the phase change $\Delta\phi_j$ should be replaced by the transmission coefficient T_j and the respective phase change [15]. Our method can be extended also to the guides of other shapes. The simplest case (the plane-parallel guide) is described by Eqs. (1)–(5) with the taper angle $\gamma=0$. To find the features of rectangular guides one should simply use the method for both the x and y coordinates. The method can be easily extended also for the polygonal guides. In the case of the curved shapes (circular, elliptical, coaxial, or arbitrary-shape guides) finding of the equivalent source is an interesting mathematical problem. In principle, it can be solved as the problem of polygonal guides with the number of sides $N\to\infty$. It should be mentioned that the correspondence between free-space modes and waveguide modes is also the basis of the nonorthogonal mode formalism derived in Ref. [16] to describe excess quantum noise in unstable resonators. In the formalism the waveguide is essentially a lens guide.

An analysis of Eqs. (1)–(5) shows that the guided waves having an arbitrary duration, field distribution, degree of coherence, and direction of propagation at the guide entrance can be generated in free space by the appropriate equivalent source. The guided waves can be produced in free space provided an appropriate launch pattern containing multiple virtual sources can be constructed. In opposition to the conventional theory of waveguides, the field at the guide entrance can satisfy neither the guide wave equation nor the boundary conditions. That gives possibility to considering not only the mode-matched waves, but also the fields having more complicated spatial and temporal properties at the guide entrance. This approach is illustrated in the following section using several particular fields, such as the diffraction-free, self-imaging, ultrashort, solitonlike, partially coherent waves and laser fractals. The fields are compared, where it is possible (mode-matched fields), to those obtained by solving a boundary condition problem.

III. PARTICULAR FIELDS

Let us consider the optical guiding and the respective free-space propagation of the several particular fields. We first demonstrate that the TEM eigenmodes $\psi_i(x,z,t)$ of the plane-parallel guide $(a=b,\gamma=0)$ having the total-reflection walls can exist and propagate without diffractive broadening not only in the optical guide but also in free space. According to the conventional theory of waveguides, the wave having the mode-matched profile and the plane wave front at the guide entrance propagates down the optical conduit as the waveguide eigenmode. In our consideration, it means that $E_0(x,z=0,t=0)=\psi_i(x)$, $R_m=1$ and $\Delta\phi_m=\pi m$. For such conditions Eqs. (1)–(5) give

$$E'(x',t)=\frac{1}{\sqrt{i\lambda/2}}\int_{-(2M+1)a}^{(2M+1)a}\frac{\exp[i(kr(x',x)-\omega t)]}{r(x',x)}\psi_i(x)dx. \tag{6}$$

The virtual source producing the waveguide eigenmode in the free space is particularly simple: $E(x,z=0)=\psi_i(x)$ for $x\in[-(2M+1)a,(2M+1)a]$ and $M=d_m/2a-1$. It should be noted that the beams $E'_m(P',t)$ with $m>M$ do not deliver the energy to the guided field in the region $x'\in[-a,a]$. Therefore, the field $E(x,z=0)=\psi_i(x)$ can be extended to the full region $x\in[-\infty,\infty]$. The interference and diffraction of this field produces the ''diffraction-free'' beam in the free space. Moreover, it can be easily demonstrated that the superposition of the eigenmodes $\psi_i(x,z,t)$ and $\psi_j(x,z,t)$ is the longitudinally periodic field with the beat length $Z_0=2\pi(k_i-k_j)^{-1}$. That means that the respective virtual source produces the self-imaging field in the free space. As an example, Fig. 2 shows the intensity distributions calculated for the eigenmode TE_0, the ''transient modes'' $E'_m(x',t)$, and the superposition of the transient modes $E'(P',t)=\Sigma_{m=|-M|}^{M}E'_m(P',t)$. We notice that the distributions of the eigenmode TE_0 and the superposition $E'(P',t)$ are indistinguishable in the ''core'' region. Figure 3 demonstrates the intensity distributions of the eigenmodes TE_1 and TE_2 and the superposition TE_1+TE_2 calculated using Eqs. (1)–(6) for the different distances z from the virtual source. The respective distributions obtained using the conventional theory of waveguides are presented in Fig. 3 for the comparison. One can see that the distributions are indistinguishable. The above presented results demonstrate the unexpected correspondence between the waveguide eigenmodes and the

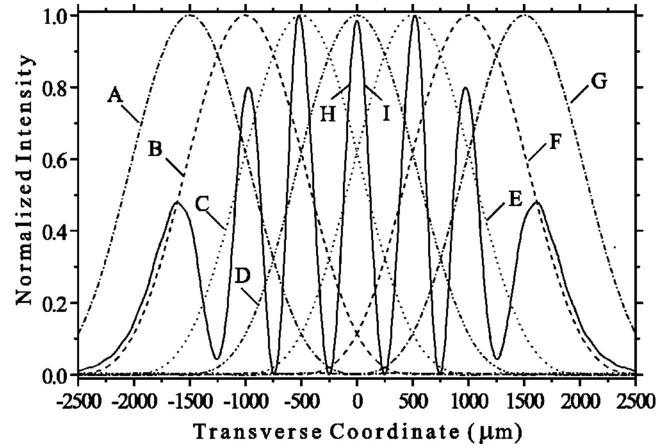

FIG. 2. The normalized intensity distributions of the eigenmode TE_0, the transient modes $E'_m(x',t)$, and the superposition of the transient modes $E'(P',t)=\Sigma_{m=|-3|}^{3}E'_m(P',t)$. Curves A, B, C, D, E, F, and G are, respectively, the normalized intensities of the transient modes having $m=-3$, -2, -1, 0, 1, 2, and 3. Curves H and I are, respectively, the normalized intensities of the TE_0 eigenmode and the superposition $E'(P',t)$ in the core region $x\in[-a,a]$). The intensity distributions of the transient modes and their superposition were calculated for the distance $z=1$ m from the virtual source using the parameters $\lambda=500$ nm and $2a=500$ μm.

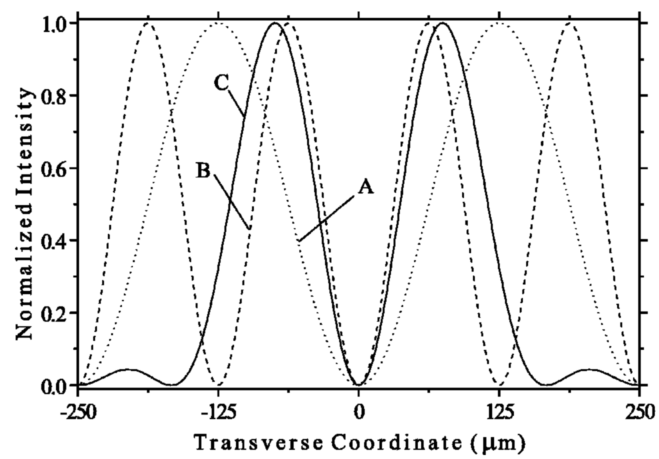

FIG. 3. The normalized intensity distributions of the eigenmodes TE_1 and TE_2 and their superposition TE_1+TE_2 calculated using Eqs. (1)–(6) for the different distances z from the virtual source. The respective distributions obtained using the conventional theory of waveguides are presented for the comparison. Curves A, B, and C show, respectively, the fields TE_1, TE_3, and TE_1+TE_3 at the guide entrance. Curves A and B demonstrate, respectively, the fields TE_1 and TE_3 computed for $z=20,21,\ldots,600$ cm. Curve C shows the field TE_1+TE_3 calculated for $z=66.6$ cm$+pZ_0$, where $p=1,2,\ldots,10$ and $Z_0=33.3$ cm. The distributions were calculated using the parameters $\lambda=500$ nm and $2a=500$ μm.

diffraction-free [1–8] and self-imaging [11–14] fields of free space. It is clear now that the diffraction-free Bessel-type beam [1–8] is the free-space equivalent of the eigenmode of the cylindrical waveguide.

Let us now consider the optical guiding and the respective free-space propagation of the field, which at the guide entrance has more complicated temporal properties. We will study an ultrashort light pulse, a wide-frequency-bandwidth field. The input pulse $E_0(x,z=0,t)$ at the guide entrance can be presented in the form of the Fourier integral

$$E_0(P,t)=\int_{-\infty}^{\infty} E_0(P,\omega)\exp(-i\omega t)d\omega. \tag{7}$$

Using Eqs. (1)–(5) for the input harmonic field $E_0(P,\omega)\exp(-i\omega t)$ and substituting the result into Eq. (7), we get the field distribution of the pulse inside the guide. A simple analysis of the equations yields a new prediction, the ultrashort wave propagates through the guide as the superposition of many pulses that diffract in the off-axis direction and interfere with each other. An example of the computer simulation of the evolution of the 10-fs pulse inside the plane-parallel hollow waveguide of the thickness $2a=2b=500$ μm and the length $z_L=10$ cm is shown in Figs. 4 and 5. At the guide entrance the Gaussian-shaped pulse matches the profile of the TE_0 or TE_3 eigenmodes and has the plane wave front,

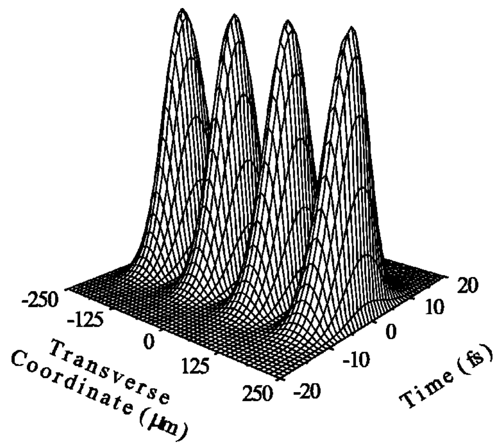

FIG. 5. The normalized intensity distributions of the pulse having $E_0(x)=TE_3(x)$ calculated using Eqs. (1)–(7) for the different distances $z=0,5,10$ cm from the virtual source. The respective distributions obtained using the conventional theory of waveguides are shown for comparison.

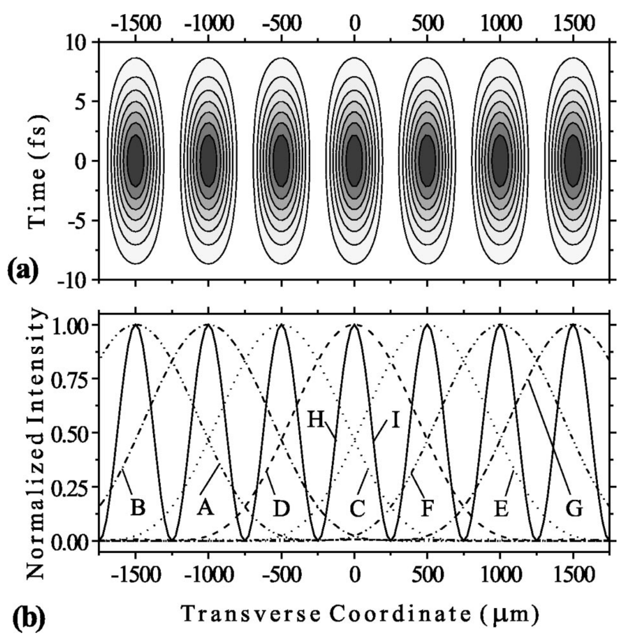

FIG. 4. (a) The normalized intensity distributions calculated for the input pulse, the transient modes $E'_m(x',t)$, and the superposition of the transient modes $E'(P',t)=\sum_{m=|-12|}^{12}E'_m(P',t)$. The input pulse matches the eigenmode TE_0. (b) Curves A, B, C, D, E, F, and G are, respectively, the normalized intensities of the transient modes having $m=-3$, -2, -1, 0, 1, 2, and 3. Curves H and I are, respectively, the normalized intensities of the TE_0 eigenmode and the superposition $E'(P',t)$ of the transient modes in the core region $x\in[-a,a]$. The intensity distributions of the transient modes and their superposition were calculated for the distance $z=0.8$ m from the virtual source. Curves A, B, C, D, E, F, G, H, and I show the intensities at the time $t=0$ fs.

$$E_0(x,z=0,t)=E_0(x)\exp[-2\ln(2)(t/\tau_0)^2]$$
$$\times\exp\{i[kz-\omega_0 t+\phi_o(x)]\}, \tag{8}$$

where $\tau_0=10$ fs, $\lambda_0=2\pi c/\omega_0=500$ nm, and $\phi_0(x)=\text{const}$. Figure 4 shows the intensity distributions calculated for the input pulse, the ''transient modes'' $E'_m(x',t)$ and the superposition of the transient modes $E'(P',t)=\sum_{m=|-M|}^{M}E'_m(P',t)$. The input pulse matches the eigenmode TE_0, $E_0(x)=TE_0(x)$. One can see that the distributions of the input pulse and the superposition $E'(P',t)$ are indistinguishable. Figure 5 shows the intensity distributions of the pulse having $E_0(x)=TE_3(x)$ calculated using Eqs. (1)–(7) for the different distances from the virtual source. The respective distributions obtained using the conventional theory of waveguides are shown for the comparison. We notice that the distributions are indistinguishable. Thus the usual result of the modal dispersion theory is recovered; the spatial profile of the wave is undistorted along its path of propagation provided the input pulse is mode matched. That means that an ultrashort pulse can exist and propagate without diffractive broadening not only in the optical guide but also in free space. It is interesting to consider also a soliton-like wave, the field that broadens neither transversely nor longitudinally. In order to derive the features of such a field, we recast the previous result for a short wave propagating in the dispersive guide $[n_1=n_1(\omega)]$. The pulse at the guide entrance is given by $E_0(x,z=0,t)=E_0(x)E_0(t)$. Using Eqs. (1)–(5) for the input field that matches the eigenmode profile $E_0(x)=\psi_i(x)$ and neglecting the unimportant proportionality factor we get the field $E'(P',t')$ at the point $P'(x')$ of the region $x'\in[-a,a]$,

$$E'(P',t')=\psi_i(x')\int_{-\infty}^{\infty}[\omega n_1(\omega)]^{1/2}E_0(\omega)\exp(-i\omega t')d\omega, \tag{9}$$

where $E_0(w)$ is the Fourier transform of the field $E_0(t')$. In the case of $\omega n_1(\omega)=\text{const}$ the pulse is a solitonlike field, which broadens neither transversely nor longitudinally. Thus a solitonlike pulse propagating inside the dispersive guide without distortion can be produced by the virtual source in the "free" space.

We now consider the optical guiding and the respective free-space propagation of the partially coherent wave. At the guide entrance, the incoherent or partially coherent wave $E_0(x,z=0,t)$ can be described in terms of the mutual coherence function $\Gamma_{00}(P^i,P^j;\tau)$ (for example, see [17]),

$$\Gamma_{00}(P^i,P^j;\tau)=\langle E_0(P^i,t+\tau)E_0^*(P^j,t)\rangle_t, \tag{10}$$

where the points $P^i,P^j\in[-a,a]$. Using Eqs. (1)–(5) and the mutual intensity function $J_{00}(P^i,P^j)=\Gamma_{00}(P^i,P^j;0)$, we get the mutual intensity $J(P'^i,P'^j)$ inside the guide

$$J(P'^i,P'^j)=\sum_{m=|-M|}^{M}\sum_{n=|-M|}^{M}\int_{x_m^{min}}^{x_m^{max}}\int_{x_m^{min}}^{x_m^{max}}J_{mn}(P_m^i,P_n^j)\times\exp[-n_1c^{-1}\omega(r_i-r_j)]\times\frac{\chi(\Theta'^i)}{r_i\lambda}\,\frac{\chi(\Theta'^j)}{r_j\lambda}dx_idx_j, \tag{11}$$

with

$$J_{mn}(P^i,P^j)=\langle E_0(P_m^i,t)E_0^*(P_n^j,t)\rangle_t, \tag{12}$$

where $\chi(\Theta)=1+\cos\Theta$; the points $P_m^i,P_m^j\in[x_m^{min},x_m^{max}]$ can be found using Eqs. (2)–(4). Using the function $J(P'^i,P'^j)$, one can easily find the complex coherence factor $\mu(P'^i,P'^j)$, the mutual coherence function $\Gamma(P'^i,P'^j)$, and the intensity distribution $I(P')=J(P'^i,P'^j;P'^i\to P'^j)$ of the guided wave [17]. In order to better understand the transformation of the guided waves into the free-space fields, we have numerically examined the guided fields having different degree of the spatial coherency. We considered the intensity distribution of the guided fields that at the guide entrance are incoherent, partially coherent, or coherent. Such fields can be produced by an incoherent, uniform-intensity, quasimonochramatic linear source placed at the different distances from the guide entrance [17]. The input fields can be described by the mutual intensity

$$J_{00}(x_i,x_j)=\int_{-h}^{h}\int_{-h}^{h}J(x_i'',x_j'')\exp[-n_0c^{-1}\omega(r_i''-r_j'')]\times\frac{\chi(\Theta''^i)}{r_i''\lambda}\,\frac{\chi(\Theta''^j)}{r_j''\lambda}dx_i''dx_j'', \tag{13}$$

with

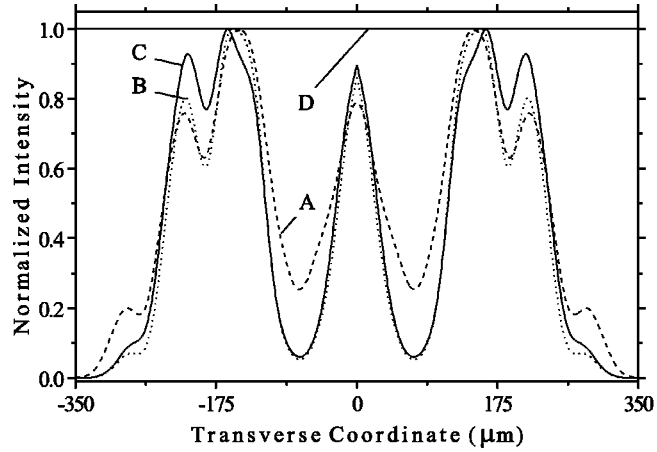

FIG. 6. Normalized intensity distributions of the partially coherent field at the guide exit computed using Eqs. (10)–(14). The parameters of the light at the guide entrance: A, $|\mu|=1$; B, $|\mu|=0.85$; C, $|\mu|=0.75$; and D, $|\mu|=0$.

$$J(x_i'',x_j'')=\sqrt{I(x_i'')I(x_j'')}\left[2\frac{\sin(2\pi\sqrt{(\Delta x'')^2}/\lambda)}{(2\pi\sqrt{(\Delta x'')^2}/\lambda)}\right]. \tag{14}$$

We computed the intensity distribution at the exit of the straight guide having the thickness $2a=2b=700\ \mu$m and the length $z_L=10$ cm. The input radiation is produced by the linear source having the length $h=125\ \mu$m and $\lambda=500$ nm. Figure 6 shows the normalized intensity for the partially coherent fields B and C. The distributions produced by the coherent A and incoherent D input fields are shown for the comparison. At the guide entrance the partially coherent fields, strictly speaking, are not the mode-matched waves. Therefore it is difficult to compare directly the calculations with that of the eigenmode theory. Nevertheless, we notice that the usual result of the theory of partially coherent fields is recovered, the spatial profile of the guided wave broadens with decreasing the coherence degree.

Finally, we consider the relation between the guided waves and the laser fractal fields. Let us consider the formation of light fields in the laser resonator, which consists of a plane-parallel waveguide, two concave mirrors, and an aperture (Fig. 7). The aperture consists of the walls of the guide

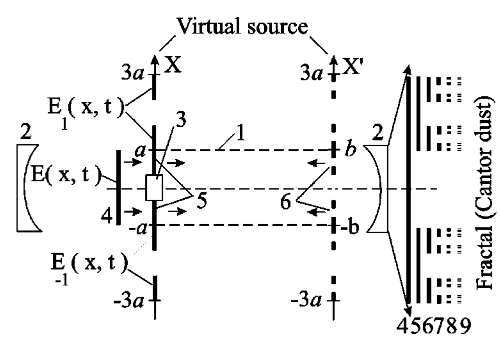

FIG. 7. Formation of the laser fractal (Cantor dust) in the waveguide resonator: 1, guide boundary; 2, mirrors, and 3, obstacle. The triadic Cantor discontinuum (line fractal): 4, C_0; 5, C_1; 6, C_2; 7, C_3; 8, C_4; and 9, C_5.

and a light obstacle placed on the laser axis at the guide entrance. The obstacle length is given by $|x|=2a/q$, where q is a natural number. The transverse dimension of the "step-like" input field E is equal to the guide thickness $2a$. The obstacle cuts the $2a/q$ part of this field creating the field E_0. Guiding of the field E_0 can be presented as propagation of the fields E'_m generated by the respective fields E_m of the virtual source [Eqs. (1)–(5)]. After reflection from the mirror, the M-times reduced image of the field $E' = \Sigma_{-|m-1|}^{m-1} E'_m$ arrives to the guide exit. In the limit of small diffraction effect [$E'_m \approx E_m$, see Eq. (1)], the round-trip process can be presented as the mathematical procedure of construction of the line fractals by the tremas [18]. In the case of $2a=1$, $q=3$, $m=(-1,0,1)$, and $M=3$, the intersection of the sets C_m is the triadic Cantor dust $C=\cap_m C_m$, the fractal with Hausdorf's dimension $D=\log 2/\log 3$. Here, $C_0 = E$, $C_1 = E_0$, and C_2 is the reduced image of the field $E' = E'_{-1} + E'_0 + E'_1$ (see Fig. 5). In order to find the set C_k one should simply repeat the round-trip procedure for the input "field" C_{k-1}. The result means that the laser fractal (triadic Cantor dust) can be generated in the free space by the waveguide resonator. The laser fractals were recently observed in the experiments [9,10]. The studies have shown that a fractal pattern can only appear if the two mirrors form a so-called unstable configuration. In our case such a configuration is formed by the two mirrors and the virtual source of the waveguide.

IV. CONCLUSION

In conclusion, it is shown using the scalar diffraction theory and the method of images that the arbitrary field confined by the optical waveguide can be generated in free space by the appropriate light source. The guided field can be produced in free space provided an appropriate launch pattern containing multiple virtual sources can be constructed. In opposition to the conventional theory of waveguides, the field at the guide entrance can satisfy neither the guide wave equation nor the boundary conditions. That gives possibility to considering not only the mode-matched waves, but also the fields having more complicated spatial and temporal properties at the guide entrance. The correspondence between the guided and free-space waves was illustrated using several particular fields, such as the diffraction-free, self-imaging, ultrashort, solitonlike, partially coherent waves and laser fractals. The fields were compared, where it was possible (mode-matched fields), to those obtained by solving a boundary condition problem. It is expected that our method can be extended to the electron and neutron waves (for the diffraction-free beams the problem was discussed in Ref. [1]).

ACKNOWLEDGMENTS

This work was supported by the Hungarian Scientific Research Foundation (OTKA, Contract No. T 026644) and in part by the U.S. Department of Energy.

[1] J. Durnin, J. J. Miceli, and J. H. Eberly, Phys. Rev. Lett. **58**, 1499 (1987).
[2] T. Wulle and S. Herminghaus, Phys. Rev. Lett. **70**, 1401 (1993).
[3] S. Klewitz, P. Leiderer, S. Herminghaus, and S. Sogomonian, Opt. Lett. **21**, 248 (1996).
[4] Z. Jaroszewicz, A. Kolodziejczyk, A. Kujawski, and C. Gomez-Reino, Opt. Lett. **21**, 839 (1996).
[5] R. Borghi and M. Santarsiero, Opt. Lett. **22**, 262 (1997).
[6] V. E. Peet and R. V. Tsubin, Phys. Rev. A **56**, 1613 (1997).
[7] D. Ding and Z. Lu, Appl. Phys. Lett. **71**, 723 (1997).
[8] S. Chavez-Cerda, M. A. Meneses-Nava, and J. Miguel Hickmann, Opt. Lett. **23**, 1871 (1998).
[9] G. P. Karman and J. P. Woerdman, Opt. Lett. **23**, 1909 (1998).
[10] G. P. Karman, G. S. McDonald, G. H. C. New, and J. P. Woerdman, Nature (London) **402**, 138 (1999).
[11] W. D. Montgomery, J. Opt. Soc. Am. **57**, 772 (1967).
[12] R. Sudol and B. J. Thompson, Opt. Commun. **31**, 105 (1979).
[13] A. W. Lohmann and J. O. Castaneda, Opt. Acta **30**, 475 (1983).
[14] G. Indebetouw, J. Mod. Opt. **35**, 243 (1988).
[15] M. Born and E. Wolf, *Principle of Optics* (Pergamon, Oxford, 1980).
[16] A. E. Siegman, Phys. Rev. A **39**, 1253 (1989).
[17] J. W. Goodman, *Statistical Optics* (Wiley-Interscience, New York, 1985).
[18] G. A. Edgar, *Measure, Topology, and Fractal Geometry* (Springer-Verlag, New York, 1994).